JOURNAL OF Applied Polymer SCIENCE

Microstructure and Shape Memory Effect of Acidic Carbon Nanotubes Reinforced Polyvinyl Alcohol Nanocomposites

Fei-Peng Du,[1,2] En-Zhou Ye,[1] Chak-Yin Tang,[3] Sun-Pui Ng,[4] Xing-Ping Zhou,[2] Xiao-Lin Xie[2]

[1]School of Materials Science and Engineering, Wuhan Institute of Technology, Wuhan 430073, China

[2]State Key Laboratory of Materials Processing and Die & Mould Technology, School of Chemistry and Chemical Engineering, Huazhong University of Science and Technology, Wuhan 430074, China

[3]Department of Industrial and Systems Engineering, The Hong Kong Polytechnic University, Hung Hom, Hong Kong, China

[4]Hong Kong Community College, The Hong Kong Polytechnic University, Hung Hom, Hong Kong, China

Correspondence to: X.-P. Zhou (E-mail: xpzhou@mail.hust.edu.cn)

ABSTRACT: Specimens of acidic multi-walled carbon nanotubes (AMWNTs) reinforced polyvinyl alcohol (PVA) nanocomposites (AMWNTs-PVA) were prepared using different amounts of AMWNTs by the traditional solution casting, involving ultrasonic wave agitation. The microstructures and tensile properties of AMWNTs-PVA were investigated by scanning electron microscopy, dynamic mechanical analysis, and quasi-static tensile testing. AMWNTs had good compatibility with PVA and dispersed evenly in the PVA matrix. The incorporation of AMWNTs improved the tensile modulus and strength of the PVA. The shape recovery testing revealed the shape recovery capacity of AMWNTs-PVA. It was observed that the recovery ratio increased, and the shape recovery rate slightly decrease with the increase of AMWNTs content. The results showed that the AMWNTs had strong interaction with the segments of the PVA and hence affected the shape recovery behavior of PVA. © 2012 Wiley Periodicals, Inc. J. Appl. Polym. Sci. 129: 1299–1305, 2013

KEYWORDS: composites; structure–property relations; stimuli-sensitive polymers

Received 17 September 2012; accepted 6 November 2012; published online 3 December 2012
DOI: 10.1002/app.38807

INTRODUCTION

Shape memory polymers (SMPs) have attracted much attention in recent years due to their potential applications in micromechanical systems and biomedical devices.[1–3] Compared with alloys and ceramic materials, SMPs have the ability to store elastic strain energy and recover large strains with quick response when subjected to external stimuli, such as temperature, pH, electric fields, magnetic fields, and solvents.[4–6] In this study, the focus is on thermally induced SMPs (TI-SMPs) due to the advantages of a simple transition process, precise control of the transition temperature, and excellent shape memory effects.[7,8] Basically, all polymeric materials have a certain shape memory effect under heating. In particular, the structures of TI-SMPs consist of hard and soft segments. The hard segments include chemical (or physical) crosslinking points and crystalline domains (or stiffness chains) which determine the permanent shape of the polymer chain network, while the crystallinity of the soft segments varies with temperature and their morphology is temperature sensitive.[9,10] When a TI-SMP attains its glass transition temperature (T_g), the soft segments can be deformed into different lengths and orientations, and the TI-SMPs can be fixed to a temporary shape after cooling below T_g. Thus, strain energy is stored in the polymer chain network. On reheating, the deformed polymer chains become mobile and the stored energy is released. As a result, the TI-SMP spontaneously returns to its original shape in which the hard segments memory.

The microstructure of a polymer is the key factor to enhance the shape memory properties.[8] Some polymers exhibit good shape memory performance according to their specific microstructures by adapting various designated ratios of hard and soft segments, such as epoxy,[11] polyisoprene,[12] and polyurethanes based SMPs.[13,14] Despite that, relatively low mechanical strength is the major drawback of SMPs, which limits the extent of useful applications.

Polyvinyl alcohol (PVA) is a type of easy-processable and biocompatible SMP. For PVA-based SMPs, the crosslinked network and undisturbed crystal domain contribute to the permanent phase, while the amorphous phase acts as the temperature sensitive phase. Its strength and shape memory behavior could be designed by changing its crosslinked degree and circumstances. Zhang and coworkers[15,16] studied the effect of using a

© 2012 Wiley Periodicals, Inc.

Applied Polymer SCIENCE

Table I. Properties of AMWNTs-PVA with CNTs Loading

CNTs loading (wt %)	0	1	2	4
Thickness (μm)	180	170	190	180
Tensile strength (MPa)	9.9	12.8	23.2	30.6
Young's modulus (MPa)	113.4	123.5	194.7	289.1
Elongation at breakage (%)	378	192	367	252

stimulating solvent on the shape memory capacity of a crosslinked PVA. The stiffness of the PVA can become higher, to achieve better serviceability, by increasing the density of the crosslinked network. However, this leads to a decrease in the crystalline domain and the weakening of its shape recovery in the dry state.[17]

Incorporation of fillers can also increase the strength and stiffness of SMPs so that the recovery stress can be improved.[7] Carbon nanotubes (CNTs) are effective fillers for improving the mechanical strength and shape recovery effect of SMPs due to their high elastic modulus, strength and aspect ratio.[18] Poulin and coworkers[17] prepared CNTs/PVA fibers with a broadened range of T_g to enhance the shape memory capacity of PVA in the dry state and found that the composites possessed better shape memory effects than pure PVA. However, fillers including CNTs, in certain circumstances, could constrain the mobility and restrict the crystallization of the soft segments of SMPs, which lead to a decrease in the recovery ratio of the SMP composites.[19] To illuminate the influence of CNTs on the shape memory effect of PVA, in this study, the newly developed PVA filled with acidic multi-walled carbon nanotubes (AMWNTs) has been prepared and the relationship between its microstructure and tensile properties as well as the shape recovery behavior is investigated.

EXPERIMENTAL WORK

Materials

PVA 1750 ± 50 (Sinopharm Chemical Reagent Beijing Co., China) was used as the adsorbate for the fabrication of the PVA nanocomposite specimens. The degree of polymerization and saponification of this PVA were 1750 ± 50 and 99%, respectively. The MWNTs of 40–60 nm diameter and 5–15 μm length were purchased from the Chengdu Organic Chemicals Co., Chinese Academy of Sciences (China). Hydrochloric acid (37 wt %), sulfuric acid (98 wt %), and nitric acid (65 wt %) were used for the acidic treatment of the MWNTs and were obtained from the Shanghai Reagents Co. (China). All chemicals were used directly as received without further purification.

Acidic Treatment of the MWNTs

The MWNTs were first treated by a mixed solution of sulfuric acid and nitric acid in a ratio of 1 : 3 for 6 h at 100°C and followed by further treatment with hydrochloric acid for 6 h at 100°C. After filtrating and washing with deionized water, the AMWNTs were dried in an oven for 24 h at 60°C.[20,21]

Preparation of AMWNTs Reinforced PVA Nanocomposites (AMWNTs-PVA)

The AMWNTs were gradually added to water in small amounts and dispersed with the aid of ultrasonic wave agitation. Subsequently, a PVA solution (6 wt %) containing CNTs was

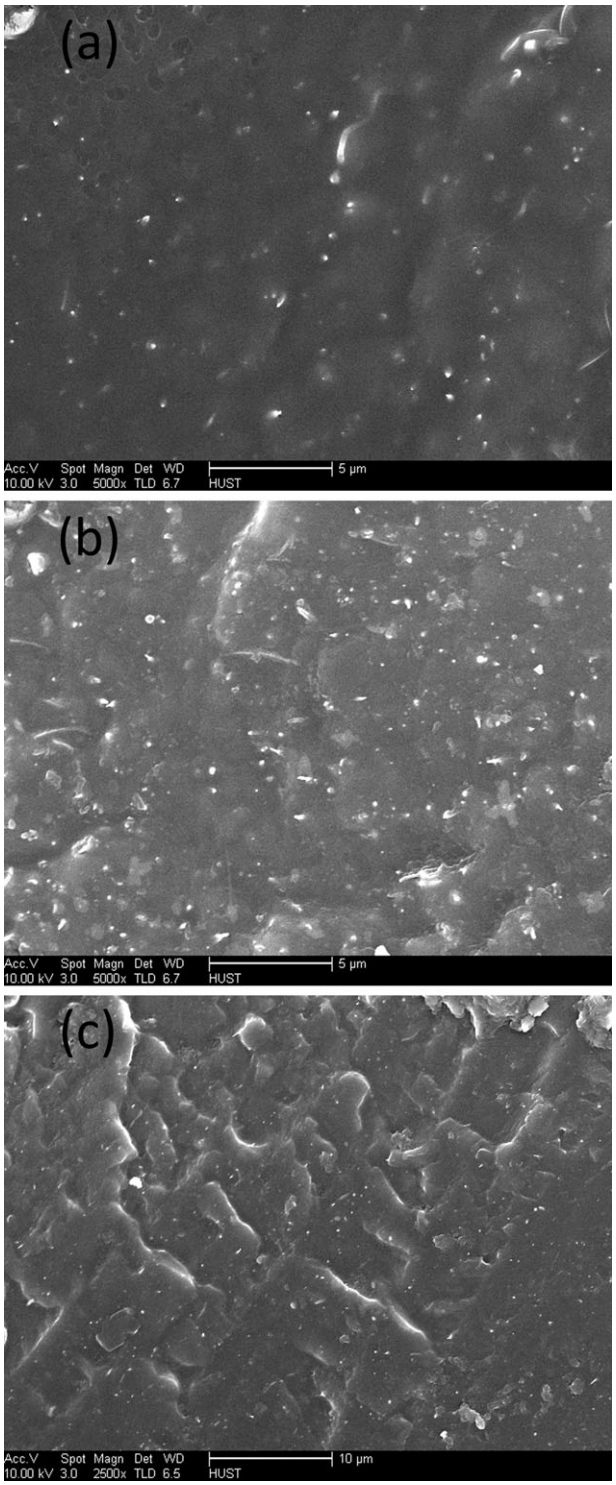

Figure 1. FESEM images of cross-section in AMWNTs-PVA membranes with the adding amounts of CNTs: (a) 1 wt %, (b) 2 wt %, and (c) 4 wt %.

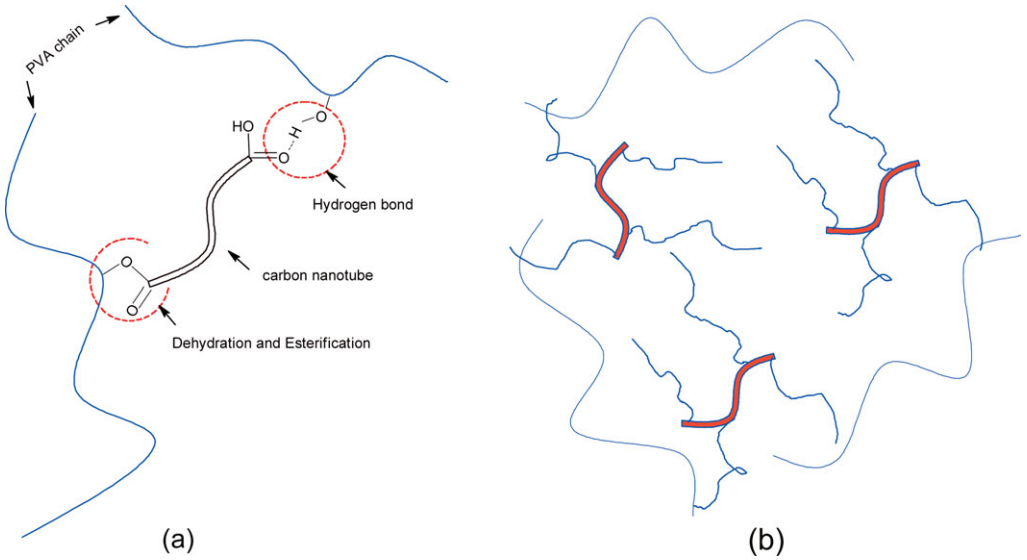

Scheme 1. Scheme of AMWNTs-PVA microstructure: (a) The interaction of CNTs and PVA chain. (b) The uniform distribution of CNTs in PVA matrix. [Color figure can be viewed in the online issue, which is available at wileyonlinelibrary.com.]

prepared by dissolving the AMWNTs in the PVA solution for 4 h at 90°C, with ultrasonic wave agitation. Finally, the AMWNTs-PVA membranes were prepared by the traditional solution casting.[22] The membrane samples were first dried naturally for 48 h at room temperature and further dried at 100°C in a vacuum oven. Test specimens were prepared as rectangular with 50 mm long and 5 mm wide by tailoring the AMWNTs-PVA membranes. The specimen thicknesses were measured using a thickness gauge and given in Table I.

Characterization

Dynamic mechanical analysis (DMA) was performed using a Perkin-Elmer Pyris Diamond DMA instrument operating at 115 V in a tensile mode. Each specimen was loaded at a fixed frequency of 1 Hz in the range of −40 to 110°C under a nitrogen atmosphere at a heating rate of 2°C/min. The microstructure at the cross-section of the membranes was observed by means of Sirion 200 field-emission scanning electron microscope (FESEM) using the liquid nitrogen cryogenic-fractured method. Quasi-static tensile tests were performed using a SANS CMT-4104 testing machine with a crosshead speed of 10 mm/min at room temperature, following the ASTM D882-02 standard for tensile properties of thin plastic sheet. The tests were performed three times for each kind of specimen. The shape recovery capacity was evaluated quantitatively using a bending test.[23] At first, the specimen was bent at 90°C and cooled down rapidly to room temperature (fixed state). It was then put in a heating chamber at a temperature of 90°C to allow shape recovery (recovery state). The original state of specimen was flat at 0°. Assuming that the bending angle in the fixed state is denoted as θ_f and that in the recovery state is θ_r, the shape recovery capacity is measured in terms of the recovery ratio R_r which is defined as $(\theta_f - \theta_r)/\theta_f \times 100\%$.[23] The recovery time was recorded as the process time from the fixed state to recovery state.

RESULTS AND DISCUSSION

Microstructures

The microstructures at the cross-sections of the AMWNTs-PVA membranes containing 1, 2, and 4 wt % of CNTs were examined from the FESEM as shown in Figure 1. The white points in each micrograph are the tips of CNTs pulled out from the PVA matrix based on the liquid nitrogen cryogenic-fracture method.[24] It can be clearly seen that CNTs were distributed evenly throughout the cross-sections of various AMWNTs-PVA membranes. More importantly, it implies that the AMWNTs have good compatibility with the PVA matrix. This excellent outcome is due to the interaction of the acidic CNTs and the PVA in nanocomposites, which is illustrated in Scheme 1.

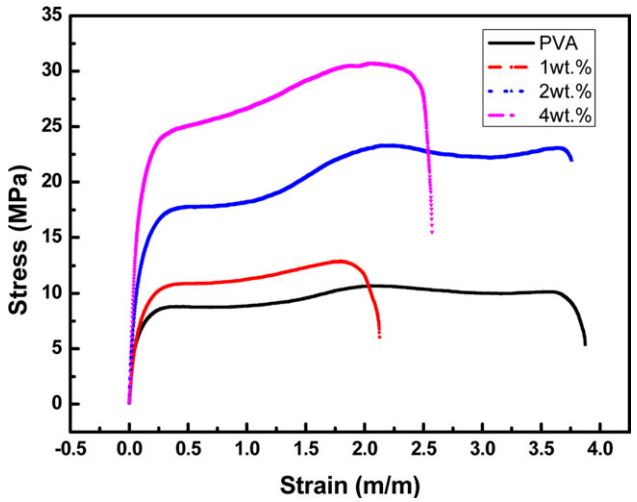

Figure 2. Tensile stress–strain curves of pure PVA and AMWNTs-PVA. [Color figure can be viewed in the online issue, which is available at wileyonlinelibrary.com.]

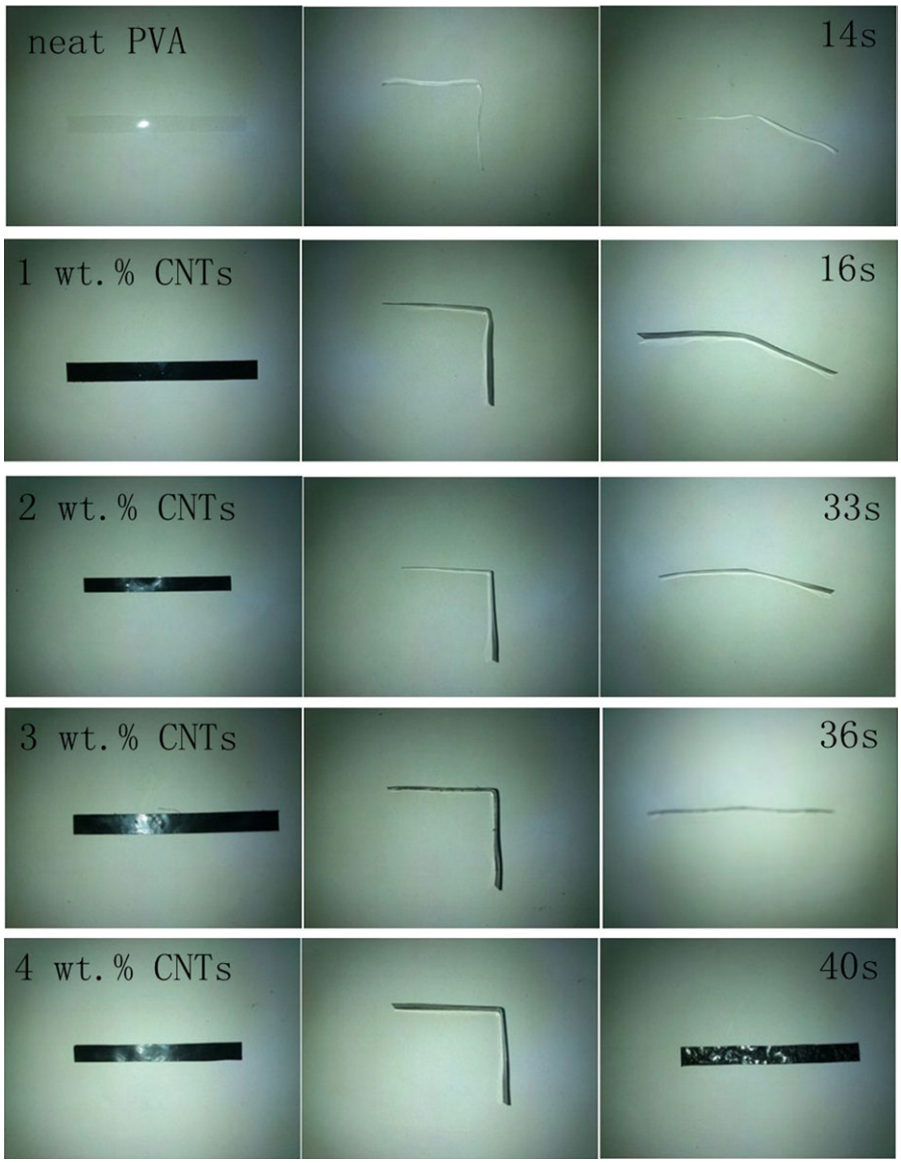

Figure 3. The shape recovery time of AMWNTs-PVA with CNTs loading. [Color figure can be viewed in the online issue, which is available at wileyonlinelibrary.com.]

During fabricating the AMWNTs-PVA membranes, the carboxylic acid groups on the surface of CNTs reacted with the hydroxyl group of the PVA by forming a hydrogen bond and/or esterification [Scheme 1(a)]. In addition to chemical bonding, the large aspect ratio of CNTs caused firm tangling with the polymer chains. Consequently, a layer of PVA molecules was attached to the surface of CNTs and thus the CNTs had good compatibility with the PVA chains and were stably dispersed in the PVA solution [Scheme 1(b)]. Therefore, the CNTs have three functions in the PVA: acting as hard segments, interacting with hard segments, and interacting with soft segments.

Quasi-Static Tensile Properties

Tensile tests were performed to evaluate the effect of CNTs loading on the tensile modulus and strength of the PVA nanocomposites. Typical stress–strain curves of the pure PVA and AMWNTs-PVA are shown in Figure 2. The tensile modulus and strength can be obtained and are listed in Table I. It can be seen that the tensile strengths of PVA nanocomposites increased gradually with the increase of CNTs loading. For example, the tensile strength of the AMWNTs-PVA specimen with 4 wt % of CNTs reached 30.6 MPa, which is about 300% as high as the pure PVA matrix strength (i.e., 9.9 MPa). A similar observation on tensile modulus was also obtained. The AMWNTs-PVA with 4 wt % of CNTs had the highest tensile modulus of 289.1 MPa, which is around 255% higher than the modulus of pure PVA matrix (i.e., 113.4 MPa). These findings indicate that the load transferred from the matrix to the reinforcing phase has been improved. Therefore, the even distribution of AMWNTs in PVA matrix, as observed in the SEM images, and the good interfacial adhesion has been proven to improve the tensile modulus and strength of the PVA matrix.

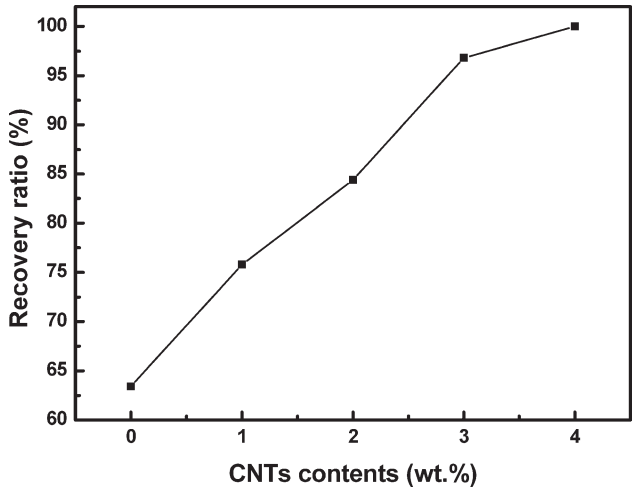

Figure 4. The relationship of recovery ratio with CNTs loading.

It is known that the inclusion of CNTs into a polymer matrix leads to a reduction in ductility of the composites.[25,26] In Figure 2, it can be observed that the elongation at breakage decreased with the addition of CNTs. Among the three AMWNT-PVA specimens containing different weights of CNTs, however, the specimen with 2 wt % of CNTs had an elongation at breakage close to that of the pure PVA specimen. The elongation at breakage values of PVA and AMWNTs-PVA can be obtained from stress–strain curves and are listed in Table I. This finding indicates that a suitable amount of CNTs can make the ductility of AMWNTs-PVA similar to that of the PVA matrix.

Shape Recovery Effect

The shape recovery capacities of AMWNTs-PVA membranes were characterized in terms of the recovery time and recovery ratio. The recovery rate can reflect the release speed of the stored strain energy in the polymer chain in the fixed state. The micro-Brownian motion of the soft segments was restricted at low temperature. However, when the temperature rises above T_g, the amorphous segments can move easily. From Figure 3, it can be seen that the recovery time was prolonged with increase of the CNTs content in the AMWNTs-PVA membranes when they was heated at 90°C. Obviously, the deformed chains of the amorphous segments in pure PVA could recover to their original shape faster than in AMWNTs-PVA. The recovery time of pure PVA was 14 s, while that of the AMWNTs-PVA with 4 wt % of CNTs increased to 40 s. The mobility of the amorphous segments in the AMWNTs-PVA had been determined by the microstructure of the nanocomposites. The CNTs had strong interaction with the amorphous chains so that the mobility of some chains was decreased. Therefore, it is found that such a hindering effect became weak when 1 wt % of CNTs was added into the AMWNTs-PVA, as the recovery time was close to that of the pure PVA matrix. On the contrary, the recovery time became relatively longer for the AMWNTs-PVA specimen with 2 wt % or more CNTs because the polymer chains required more time to unwrap and recover in the AMWNTs-PVA with presence of CNTs.

An excellent shape memory material should have a shape recovery ratio larger than 90%.[9] Figure 4 shows that the recovery ratio of the AMWNTs-PVA increases linearly with the CNTs content. The recovery ratio of pure PVA was 63.4%, while the recovery ratios of AMWNTs-PVA were larger than 90% when the CNTs contents were above 2 wt %. Particularly for the

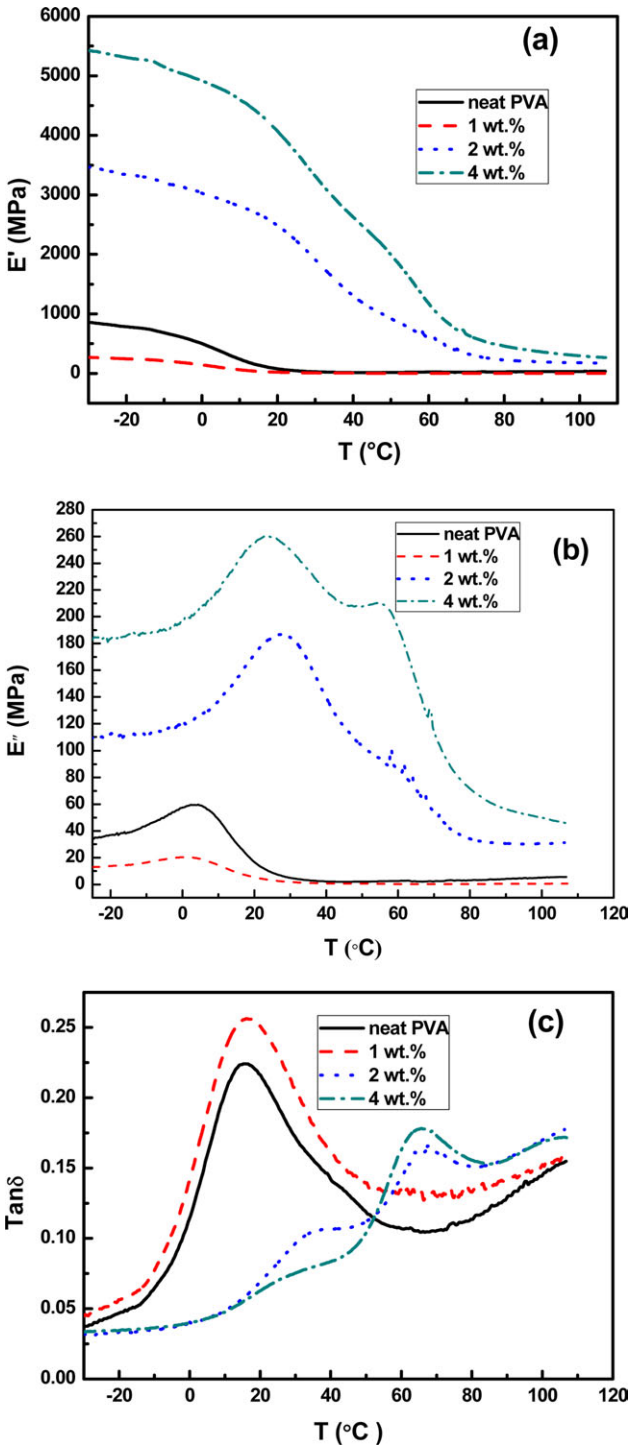

Figure 5. (a) Storage modulus, (b) loss modulus, and (c) tan δ curves of AMWNTs-PVA membranes with CNTs loading. [Color figure can be viewed in the online issue, which is available at wileyonlinelibrary.com.]

AMWNTs-PVA with 4 wt % of CNTs, the recovery ratio nearly reached 100%. The hard segments in the PVA controlled the shape recovery ratio.[9,27] The decrease in the ratio of the hard segments to soft segments in the microstructure of the polymer lead to a decrease in the recovery ratio.[23] Moreover, some researches indicated that the micro or nano-fillers have a strong effect on reducing the mobility of the soft segments during crystallization. As a result, the crystallization of the soft segments was restricted and the corresponding recovery ratio of the SMP composites decreased.[19] For the AMWNTs-PVA in this study, the acidic CNTs had comparable sizes with the PVA hard segments, so the CNTs acted as if they were the hard segments. Therefore, AMWNTs-PVA with a higher content of CNTs was exhibiting higher shape recovery ratios.

Dynamic Mechanical Properties

The dynamic mechanical properties of PVA homopolymer and the AMWNTs-PVA membranes are shown in Figure 5. The evolution of storage modulus (E') with temperature for the different systems is shown in Figure 5(a). Over the whole temperature range of measurement, the E' of AMWNTs-PVA composites with 2 and 4 wt % of CNTs were higher than that of the one with 1 wt % of CNTs and the pure PVA. From the selected values of storage modulus at about 40°C, it can be seen that the E' of the AMWNTs-PVA with 4 and 2 wt % of CNTs were 2.63 and 1.31 GPa, respectively, while the E' of pure PVA and the AMWNTs-PVA with 1 wt % was only about 15.8 MPa. According to this great improvement of the E' of AMWNTs-PVA, it is postulated that the CNTs had strong covalent bonding with the PVA matrix. On the other hand, maximum loss modulus (E'') of AMWNTs-PVA composites with 2 and 4 wt % of CNTs were higher than that of the composite with 1 wt % of CNTs and the pure PVA, indicating that CNTs contributed towards a greater viscous response due to the interfacial mechanical friction loss [Figure 5(b)] between nanotubes and polymer matrix. Moreover, the loss modulus peak temperatures of AMWNTs-PVA composites with 2 and 4 wt % of CNTs shifted toward higher temperature indicating more restricted mobility of the PVA chains.

Figure 5(c) shows the evolution of the loss factor (tan δ) with temperature. From the plots, the tan δ peak for pure PVA is measured to be about 15 °C, whereas for AMWNTs-PVA, the location of peaks changed according to the CNTs content. These peaks correspond to the glass transition of the amorphous domains of PVA chains and the maximum peak is assigned as the glass-transition temperature (T_g). As shown in Figure 5(c), T_g moves to a higher temperature as the amount of CNTs increases. Furthermore, the AMWNTs-PVA composites with 2 and 4 wt % of CNTs had lower values of tan δ at T_g. It is obvious that the intensity of the transition decreases when CNTs more than 2 wt % was incorporated into the PVA matrix. These findings also imply that the CNTs had strong interaction with the PVA matrix, which enhanced the interfacial adhesion and restricted the motion of the PVA chains.[28,29]

Additionally, the E' of the AMWNTs-PVA with 2 and 4 wt % of CNTs decreased more than one order when the temperature rose to the glass transition region which is considered the most significant condition for rendering the shape memory behavior of materials.[30] With a large elasticity difference, high temperature deformation becomes easier while maintaining a high resistance to deformation at low temperature.[9,13] Therefore, the external energy was stored effectively in the structure below T_g, and released completely above T_g. These facts can further prove that the presence of compatible CNTs in the PVA polymer enhanced its shape recovery ratio and stress.

CONCLUSIONS

AMWNTs-PVA was prepared by traditional solution casting and the uniformity of the CNTs in the PVA matrix was ensured by the ultrasonic wave agitation. Acidic CNTs had good compatibility with PVA matrix and were distributed evenly in the PVA matrix. Uniform CNTs caused AMWNTs-PVA to have high tensile strength and modulus, and these properties varied with the increasing amount of CNTs. Acidic CNTs had strong interaction with both the hard and soft segments. The two different of shape recovery effects were demonstrated with the increase of CNTs loading: the decrease in recovery rate due to the restriction of the soft segment mobility, and the increase in recovery ratio due to the presence of CNTs and their interaction with the PVA hard segments.

ACKNOWLEDGMENTS

This work was supported by the National Natural Science Foundation of China (50903034 and 51035002) and the Research Committee of The Hong Kong Polytechnic University (G-U844).

REFERENCES

1. Lu, X. L.; Cai, W.; Ga, Z. Y. *J. Appl. Polym. Sci.* **2008**, *108*, 1109.
2. Meng, Q. H.; Hu, J. L.; Zhu, Y.; Lu, J.; Liu, Y. *Smart Mater. Struct.* **2007**, *16*, 1192.
3. Zhang, Q.; Yang, Q. S. *J. Appl. Polym. Sci.* **2012**, *123*, 1502.
4. Chung, T.; Uribe, A. R.; Mather, P. T. *Macromolecules* **2008**, *41*, 184.
5. Xie, T.; Rousseau, I. A. *Polymer* **2009**, 50, **1852**.
6. Zhang, C. S.; Ni, Q. Q.; Fu, S. Y.; Kurashiki, K. *Compos. Sci. Technol.* **2007**, *67*, 2973.
7. Ohki, T.; Ni, Q. Q.; Ohsako, N.; Iwamoto, M. *Compos. Part A Appl. Sci. Manuf.* **2004**, *35*, 1065.
8. Hearon, K.; Gall, K.; Ware, T.; Maitland, D. J.; Bearinger, J. P.; Wilson, T. S. *J. Appl. Polym. Sci.* **2011**, *121*, 144.
9. Liu, G. Q.; Guan, C. L.; Xia, H. S.; Guo, F. Q.; Ding, X. B.; Peng, Y. X. *Macromol. Rapid Commun.* **2006**, *27*, 1100.
10. Razzaq, M. Y.; Anhalt, M.; Frormann, L.; Weidenfeller, B. *Mater. Sci. Eng. A Struct. Mater.* **2007**, *471*, 57.
11. Liu, Y. P.; Gall, K.; Dunn, M. L.; McCluskey, P. *Mech. Mater.* **2004**, *36*, 929.
12. Liu, C. D.; Chun, S. B.; Zheng, P. T. M.; Haley, E. H.; Coughlin, E. B. *Macromolecules* **2002**, *35*, 9868.
13. Kim, B. K.; Lee, S. Y.; Xu, M. *Polymer* **1996**, *37*, 5781.

14. Kim, B. K.; Lee, S. Y.; Lee, J. S.; Baek, S. H.; Choi, Y. J.; Lee, J. O.; Xu, M. *Polymer* **1998**, *39*, 2803.

15. Du, H.; Zhang, J. *Soft Matter* **2010**, *6*, 3370.

16. Du, H.; Zhang, J. *Colloid Polym. Sci.* **2010**, *288*, 15.

17. Miaudet, P.; Derré, A.; Maugey, M.; Zakri, C.; Piccione, P. M.; Inoubli, R.; Poulin, P. *Science* **2007**, *318*, 1294.

18. Ni, Q. Q.; Zhang, C. S.; Fu, Y. Q.; Dai, G. Z.; Kimura, T. *Compos. Struct.* **2007**, *81*, 176.

19. Gunes, I. S.; Cao, F.; Jana, S. C. *Polymer* **2008**, *49*, 2223.

20. Du, F. P.; Tang, C. Y.; Xie, X. L.; Zhou, X. P.; Tan, L. *J. Phys. Chem. C* **2009**, *113*, 7223.

21. Du, F. P.; Wu, K. B.; Yang, Y. K.; Liu, L.; Gan, T.; Xie, X. L. *Nanotechnology* **2008**, *19*, 085716.

22. Tsuji, H.; Ikada, Y. *Polymer* **1999**, *40*, 6699.

23. Lin, X. K.; Chen, L.; Zhao, Y. P.; Dong, Z. Z. *J. Mater. Sci.* **2010**, *45*, 2703.

24. Cui, W.; Du, F. P.; Zhao, J. C.; Zhang, W.; Yang, Y. K.; Xie, X. L.; Mai, Y. W. *Carbon* **2011**, *49*, 495.

25. Meincke, O.; Kaempfer, D.; Weickmann, H.; Friedrich, C.; Vathauer, M. *Polymer* **2004**, *45*, 739.

26. Miyagawa, H.; Drzal, L. T. *Polymer* **2004**, *45*, 5163.

27. Liu, G. Q.; Ding, X. B.; Cao, Y. P. *Macromol. Rapid Commun.* **2005**, *26*, 649.

28. Mai, Y. W.; Yu, Z. Z. Polymer Nanocomposites; Woodhead Publishing Limited: Cambridge, **2006**; pp 540–570.

29. Liu, L. Q.; Barber, A. H.; Nuriel, S. *Adv. Funct. Mater.* **2005**, *15*, 975.

30. Tsai, Y.; Tai, C. H.; Tsai, S. J.; Tsai, F. *J. Eur. Polym. J.* **2008**, *44*, 550.